

Delta-doped CCDs: High QE with long-term stability at UV and visible wavelengths

Shouleh Nikzad, M.E. Hoenk, P.J. Grunthaner, R.W. Terhune, and F.J. Grunthaner
Center for Space Microelectronics Technology
Jet Propulsion Laboratory, California Institute of Technology, Pasadena, CA 91109

R. Winzenread, M. Fattahi, Hsin-Fu Tseng
EG&G Reticon, Sunnyvale, CA 94086.

M. Lesser
Steward Observatory, University of Arizona, Tucson, Arizona, 85721

Abstract

Delta-doped CCDs, developed at JPL's Microdevices Laboratory, have achieved stable 100% internal quantum efficiency in the visible and near UV regions of the spectrum. In this approach, an epitaxial silicon layer is grown on a fully-processed commercial CCD using molecular beam epitaxy. During the silicon growth on the CCD, 30% of a monolayer of boron atoms are deposited on the surface, followed by a 15 Å silicon layer for surface passivation. The boron is nominally incorporated within a single atomic layer at the back surface of the device, resulting in the effective elimination of the backside potential well. The measured quantum efficiency is in good agreement with the theoretical limit imposed by reflection from the Si surface. Enhancement of the total quantum efficiency in the blue visible and near UV has been demonstrated by depositing antireflection coatings on the delta-doped CCD. Recent results on antireflection coatings and quantum efficiency measurements are discussed.

1. Introduction

High resolution charge-coupled devices (CCDs) with high UV quantum efficiency (QE) have many applications in space and ground-based astronomy. The short absorption length of photons in the frontside structure of the CCD makes frontside-illuminated CCDs unresponsive in the UV. Two possible ways of making UV-responsive frontside-illuminated CCDs have been demonstrated: One is through structural modification, i.e., virtual phase CCDs¹, and the other is by using a phosphor to convert UV into visible light,² e.g., lumogen-coated frontside CCDs. While backside-illuminated, thinned CCDs offer the possibility of obtaining high UV quantum efficiency, detecting UV photons in a silicon CCD is complicated by the short absorption length of UV photons in silicon (e.g., 4 nm absorption length at 270 nm) and the existence of a backside potential well (caused by positive charge at the interface between Si and SiO₂). Treating the back surface of the CCD by negative-surface charging (i.e., UV-flooding, bias flash-gating) or ion implantation, has yielded reasonable or high UV quantum efficiency. However, these treatments suffer variously from problems of yield, response stability, hysteresis, and long-term reliability. Stability of the quantum efficiency has great impact on ground and space-based astronomy. A device with stable quantum efficiency is particularly important in space-based astronomy where renewal of the back surface treatment (e.g., by exposing the device to intense UV light) is not an attractive option.

Molecular beam epitaxy (MBE) promises a significant enhancement of imaging device technology. Nanometer-scale dopant profiles, not accessible with ion implantation or diffusion processes, could expand the range of the performance of existing devices. Using MBE, delta-doped CCDs with 100% internal quantum efficiency in the visible and

near UV were developed at Jet Propulsion laboratory.³ Fully-processed Reticon 5 12x5 12 devices were modified by low temperature molecular beam epitaxy by depositing 25 Å of delta-doped silicon on the back surface of the thinned CCDs. The quantum efficiency achieved by this method not only exceeds that of other reported treatments of backside-thinned CCDs, but also results in a stable response. The external or total quantum efficiency of these devices is limited by the reflection of photons from the silicon surface and, for photons in the far UV, absorption in the native oxide. In this paper, we will describe the delta-doping process, and the resulting quantum efficiency, uniformity, and stability of delta-doped CCDs. Further enhancement of the total or external UV response of delta-doped CCDs was demonstrated by depositing antireflection (AR) coatings on the CCD back surface.

2. Delta-doped CCD processing

MBE is used to grow epitaxial silicon on the CCD back surface with a thickness of only a few atomic layers, containing an extremely high concentration of p-type dopant atoms. This provides the necessary band bending at this interface so that the photoelectrons produced are not trapped near the interface and are instead captured in the intended front potential well.

The delta-doped CCD process is possible due to the existence of low-temperature MBE technology for growing ultra-thin, highly-doped silicon at temperatures which will not damage a CCD. In the case of Reticon CCDs, spiking of the Al contacts into the underlying silicon will damage the CCD at temperatures exceeding 500°C. During the *in situ* preparation of the device and the growth, the device temperature is never raised beyond 450°C. The device is held at 450°C only for four minutes. At this temperature, boron does not diffuse and forms an extremely thin layer of negative charge 5 Å below the Si/SiO₂ interface.

The details of the process are described in a previous paper.⁵ The main steps are as follows. Fully-processed Reticon CCD die, complete with aluminum contacts, are thinned to 15 microns at EG&G Reticon. The thinning process leaves a gold-covered thick frame around the active area of the device. As a first step the gold is chemically removed and the device is sequentially cleaned by a series of acids, bases, and solvents to remove contaminants introduced in the gold-removal process. UV-generated ozone is used to remove any remaining hydrocarbon contamination. The thin oxide (~15 Å) on the CCD back surface is then removed under N₂ atmosphere by spinning the device at 4000 rpm and dispensing an HF/ethanol solution on the surface. This process results in an atomically clean silicon surface in which the surface atoms are bound to hydrogen atoms. The CCD is then immediately loaded into the MBE chamber and is annealed at low temperature (200°C) for ~5 minutes to remove any physisorbed contaminants. The sample is finally heated to 450°C a few minutes before the growth. The layer structure consists of 10 Å of doped Si, followed by deposition of 2×10^{14} B/cm², and a final 15 Å layer of undoped silicon. Growth of this layer structure is completed in three minutes. Following the MBE growth, the back surface of the device is oxidized by a 30-minute exposure to steam. The delta-doped CCDs are then sent to Reticon for packaging and testing. This process was recently simplified by the development at Reticon of a dielectric masking material for the thinning process⁴, which eliminates the gold-removal step in preparing CCDs for the MBE growth.

Figure 1 is a high-resolution cross-sectional transmission electron micrograph of a silicon substrate with a delta-doped structure consisting of a 10 Å of doped Si, followed by

deposition of 2×10^{14} B/cm², and a final 40 Å layer of undoped silicon. In this structure the delta layer is buried deeper below the interface than for the actual CCD modification to enhance our capability to observe defects generated by the presence of this layer. Figure 1 shows that the original substrate is indistinguishable from the epilayer and there are no defects either at the substrate-epilayer interface or the delta layer. Note that, unlike ion implantation, no annealing must be performed on the lattice after the MBE process to incorporate the boron in the lattice or remove damage.

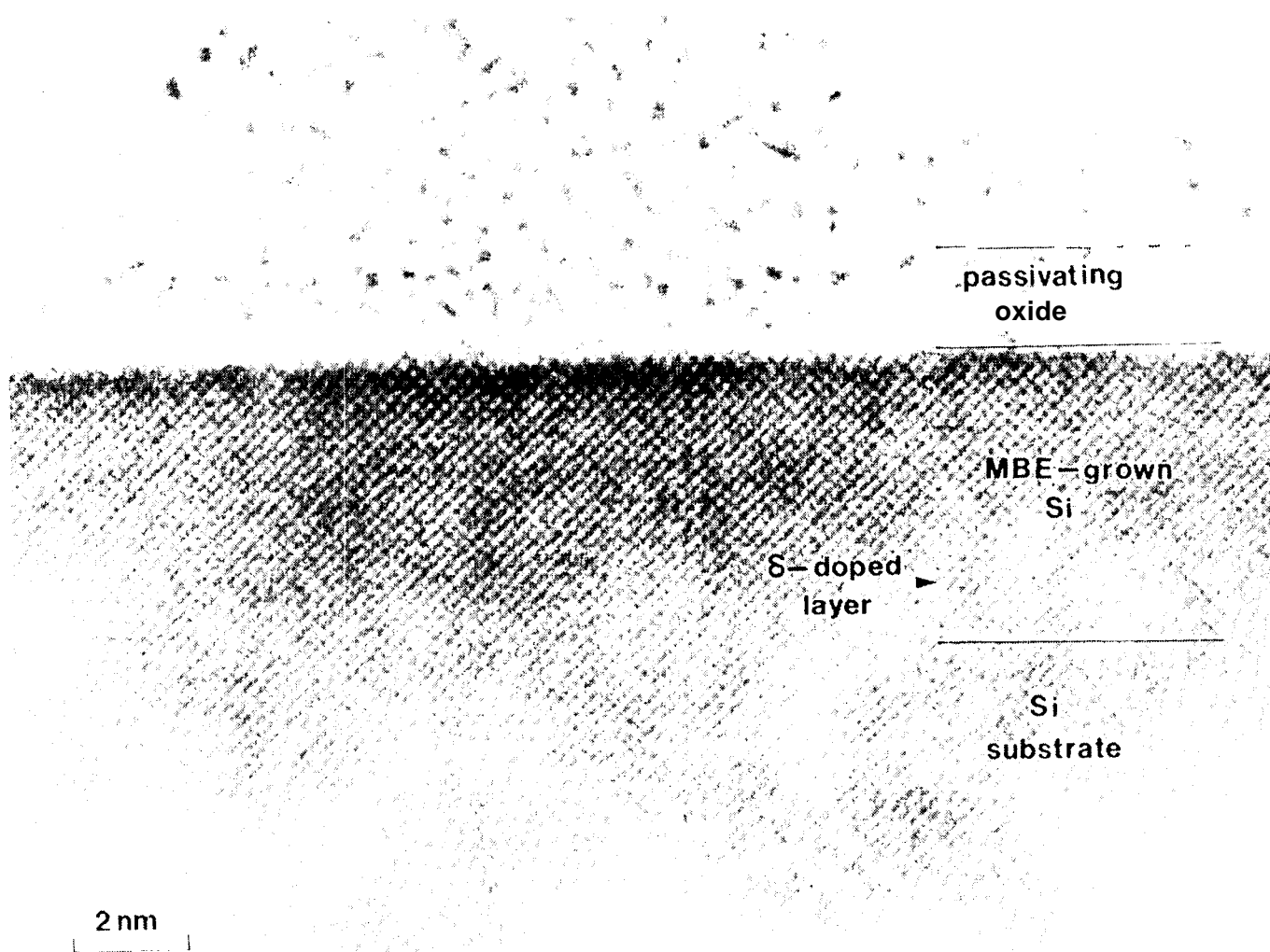


Figure 1. High-resolution cross-sectional transmission electron micrograph of a delta-doped layer grown on silicon substrate. The grid pattern in the image represents individual columns of atoms. The epilayer is indistinguishable from the original lattice indicating that the defect density is extremely low.

In the MBE process, Si deposition is performed by electron beam evaporation which produces x rays which have the potential of damaging the device. However, the total x-ray dose received during the MBE modification of the CCD is about 6 krad, which is significantly below the damage threshold of the device. Our results have not shown evidence of damage to the CCD. If necessary, electron beam evaporation can be replaced by thermal evaporation of silicon to avoid exposure of the CCDs to x rays.

3. Quantum Efficiency of the device in UV and visible

Figure 2 shows the quantum efficiency of two delta-doped CCDS measured at EG&G Reticon. The solid line is the reflection-limited quantum efficiency which is equal to the silicon transmittance. It corresponds to 100% internal quantum efficiency (number of photo-electrons equals the number of absorbed photons). As shown in Fig. 2, any photons that are not lost due to reflection from the silicon surface are detected in the delta-doped CCD. Preliminary measurements at shorter wavelengths (120-250 nm) show that the quantum yield (formation of multiple electron-hole pairs per incident photon) contributes to an increase of the quantum efficiency.

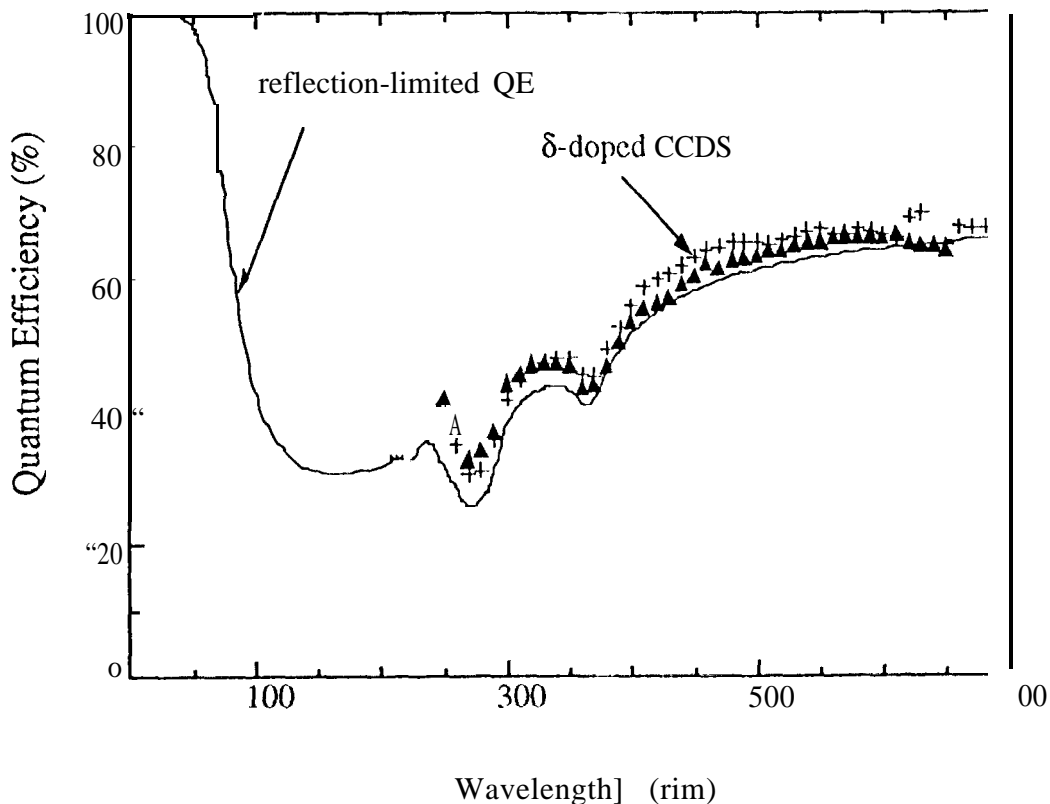


Figure 2. Quantum efficiency of two delta-doped CCDs. Comparison with the reflection-limited quantum efficiency (transmittance of silicon) shows that the delta-doped treatment achieves 100% internal quantum efficiency within the uncertainty of the measurement ($\pm 5\%$).

4. Uniformity of Response

Figure 3 shows the flat field response of a delta-doped CCD at 350 nm. The flat field response of the device is highly uniform, and the few blemishes are well within the normal range for this grade of CCD. Figure 4 is a line plot of the delta-doped CCD, again indicating that the uniformity is typical of CCDS without the MBE enhancement. Since these devices can only be tested after packaging, it is impossible to directly compare defect density and uniformity before and after the MBE growth.

The spectral uniformity of the device response was examined by measuring the quantum efficiency of a delta-doped CCD in three 50x50 pixel areas. As shown in Fig. 5, the measured spectral response is identical in these three regions. The inset in the figure shows the approximate position of the three test areas in the array. These measurements were done at the same time, under identical conditions. The pixel-to-pixel variation of the response within each test region is about 1-2%, which is typical of Reticon CCDS prior to the MBE modification.

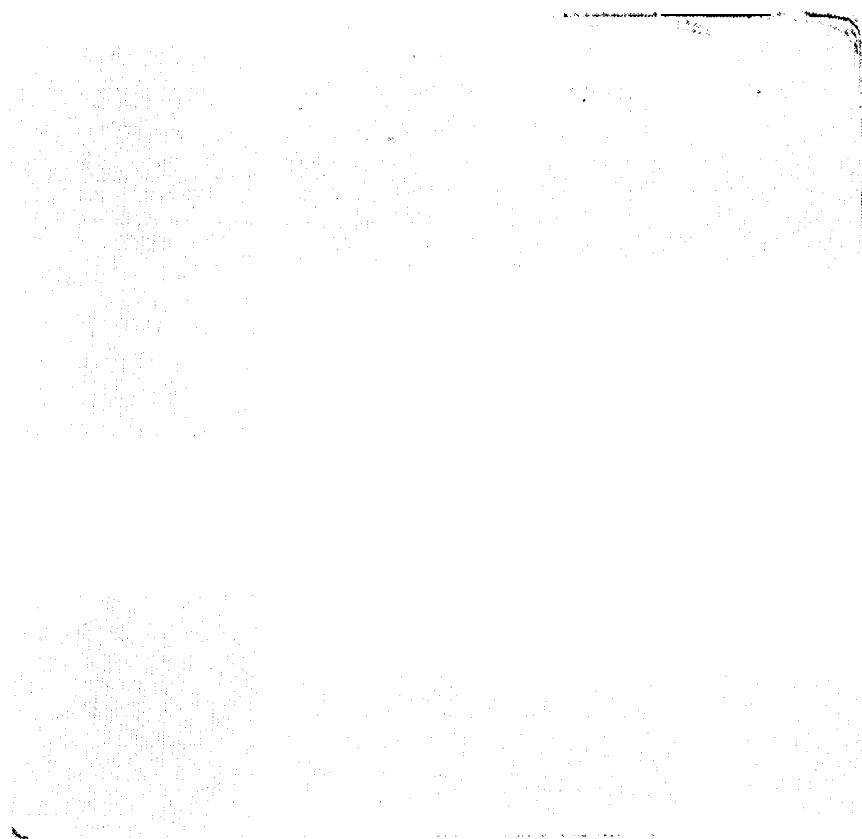


Figure 3. Flat field response of a delta-doped Reticon 512x512 CCD. This flat field response is taken at 350 nm.

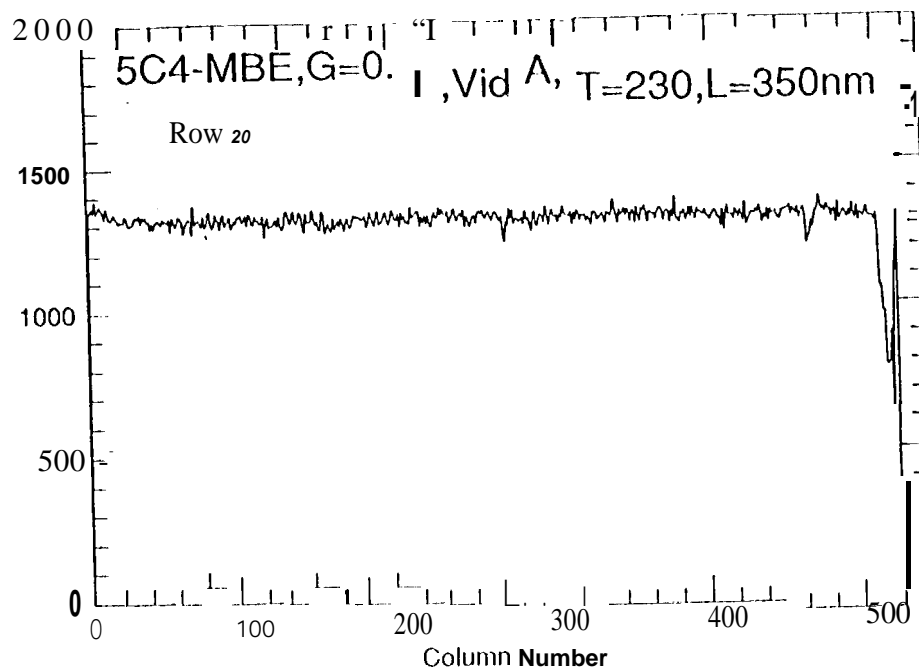


Figure 4. A typical line plot of delta-doped CCD at 350 nm.

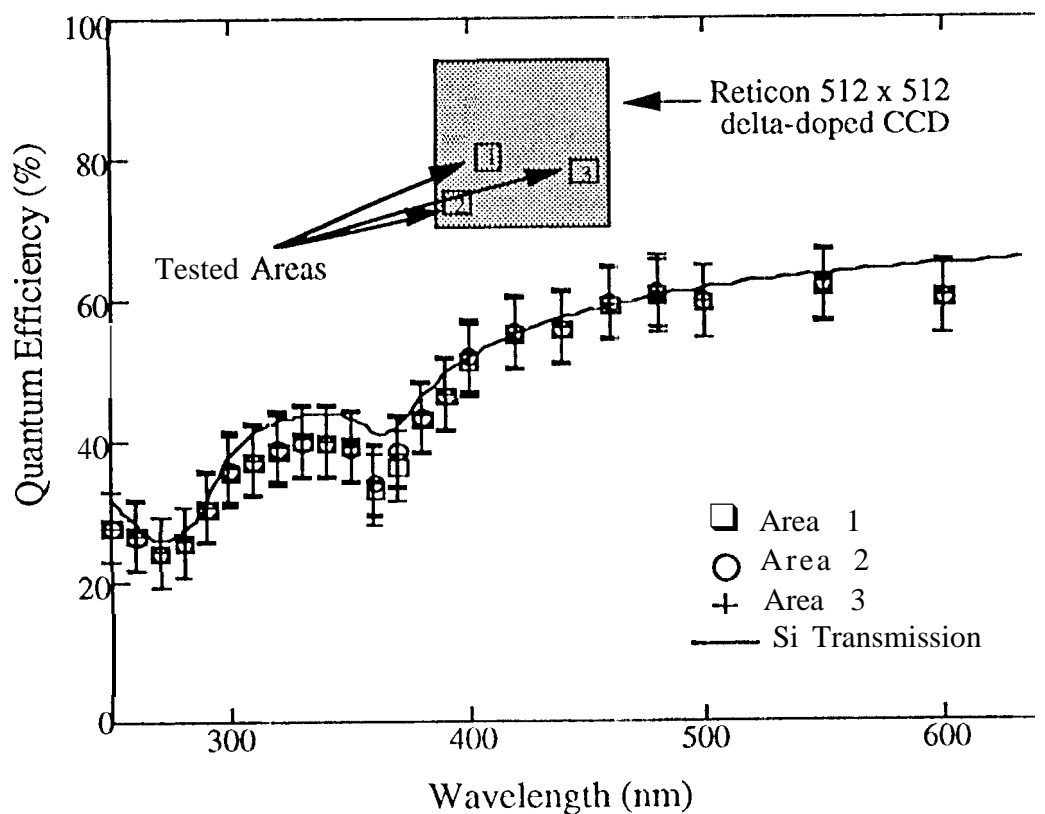


Figure 5. Spectral uniformity of delta-doped CCD measured on three 50x50 pixel areas on the device. The response in these three regions is identical.

5. Stability of the delta-doped CCD

Delta-doped CCDS have been characterized in different measurement setups and have all reported the same 10(MO internal quantum efficiency. During intervals between QE measurements and deposition of antireflection coatings, the devices have been stored in atmosphere in an antistatic box with no further protection. Sixteen months after the MBE process, and after exposure to three different vacuum and camera systems, the quantum efficiency of one of these devices was again measured. Figure 6 exhibits the original and the latest measurements on the device. It should be noted that the two measurements were performed on different systems which each claim about $\pm 5\%$ precision. Within the accuracy of the measurement, the device has shown *no* change from the ideal UV response. Although the difference between the two measurements is slightly more enhanced in the shorter wavelengths, this is most likely due to surface contamination from exposures to various systems. Note that unlike UV flooding, no repeat of the backside treatment has been required and the device performance shows no sign of degradation, despite repeated temperature cycling and exposure to different environments.

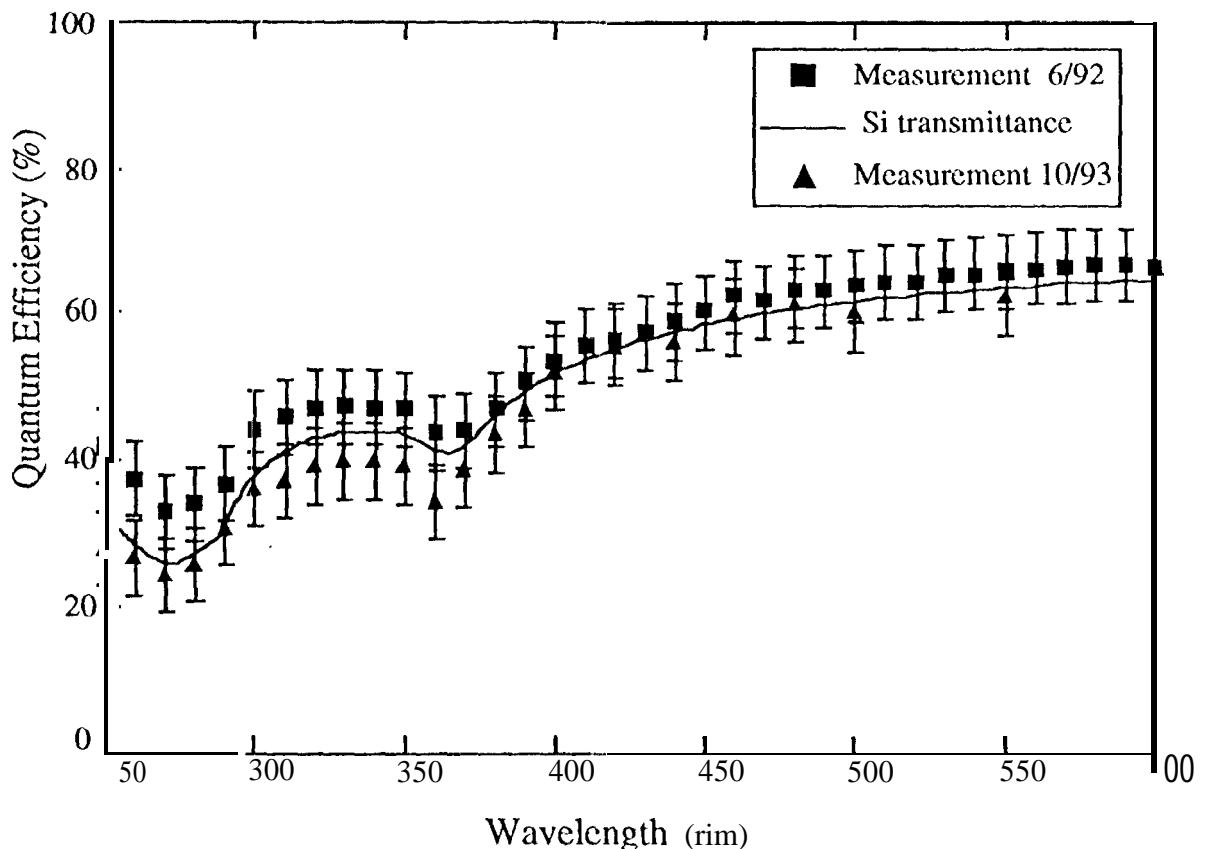


Figure 6. Measurements of a delta-doped CCD made 16 months apart in two different systems show consistent 100% internal quantum efficiency within the limits of uncertainty.

6. AR coatings on the Delta-doped CCD

The delta-doped CCD treatment permanently pins the backside potential bands by incorporating a high concentration of negative charge (boron atoms) into the silicon lattice. This charge is then protected by a thin SiO_2 layer. This technology is compatible with direct deposition of **antireflection** layers. Also, unlike other backside treatments, **antireflection** coatings for delta-doped CCD do not serve the additional purpose of surface charging which restricts the nature of layers that can be deposited. 10 demonstrate the feasibility of AR-coated delta-doped CCDs, single-layer HfO_2 coatings optimized for two different regions of the spectrum have been deposited directly on the back surface (Fig. 7). The 300-400 nm region was chosen for interest to ground-based UV astronomy applications, and 270 nm was chosen as the region of lowest response for uncoated CCDs. While single layer coatings do not provide narrow-bandpass filters, a local maxima can be obtained at 270 nm by using the appropriate thickness. The layer optimized for 300-400 nm provides a broader peak in the response, due to the smoother variation of the silicon optical constants in this region. HfO_2 layers were deposited in University of Arizona's Steward observatory CCD laboratory, using resistive heating evaporation which avoids the x-ray exposure encountered in e-beam methods.⁵ During the deposition, the CCDs are cooled to -100°C to prevent damage from radiative heating.

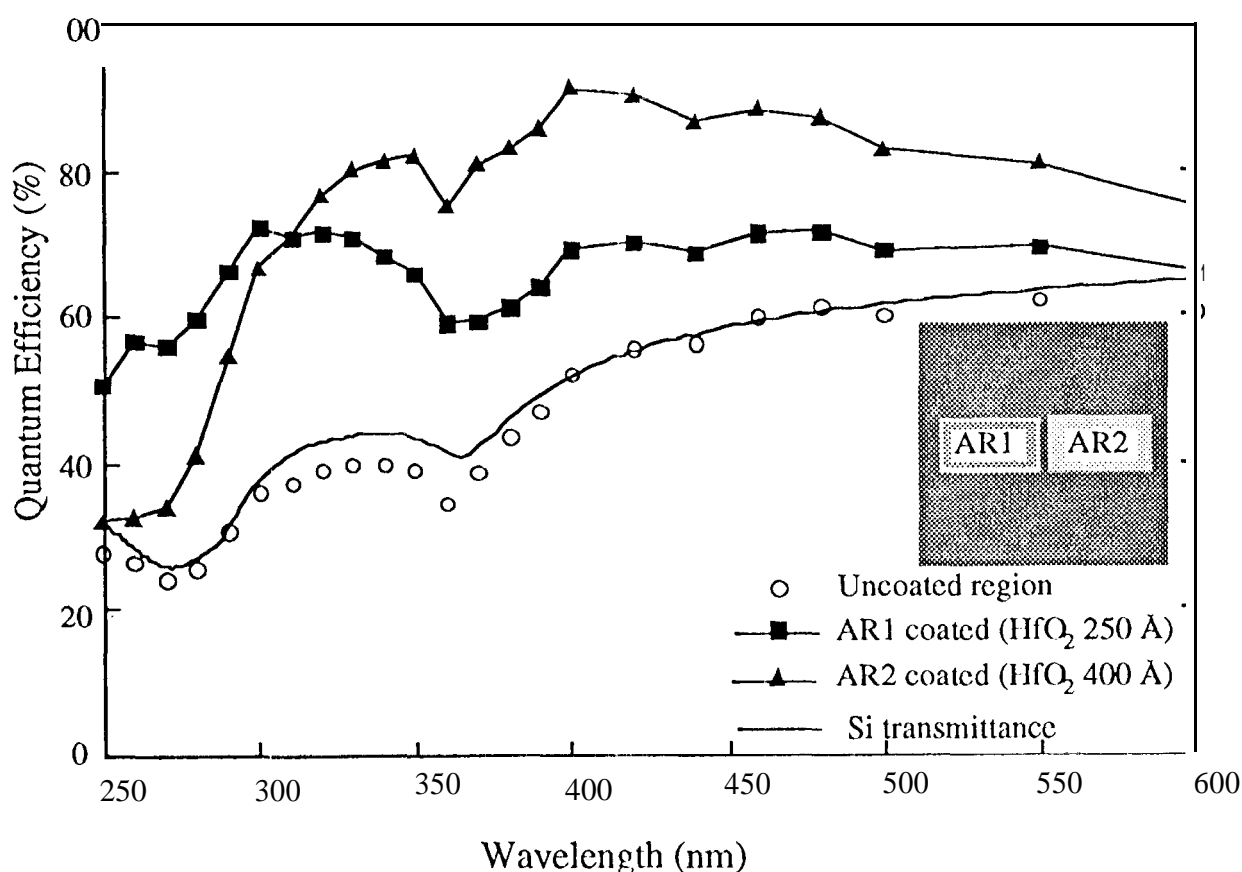


Figure 7. Quantum efficiency data from AR-coated regions of a delta-doped CCD. Two $3 \times 5 \text{ mm}^2$ areas were coated with HfO_2 (250 Å and 400 Å respectively). Data from the uncoated area of the CCD are shown for comparison.

The AR layers were deposited on small areas of packaged delta-doped CCDs. Using a shadow-masking technique, two separate $3 \times 5 \text{ mm}^2$ areas (equivalent of 111×185 pixels) were used for the deposition of the two films (400 Å and 250 Å thick). The rest of the CCL) was masked with an Al plate for control purposes. Prior to loading the CCDs in the AR deposition chamber, packages were wiped clean by xylene and isopropyl alcohol, and the devices were slowly dipped in 60°C xylene and isopropyl alcohol to remove hydrocarbons from the back surface of the CCD. Figure 7 shows the response of the delta-doped CCD in the AR-coated and uncoated areas on the same CCD, together with the theoretical uncoated silicon transmittance curve. The response of the AR-coated regions show the expected enhancement in the quantum efficiency. The uncoated regions (open circles) still respond at the theoretical reflection-limit for bare silicon, indicating that the additional AR coating processes did not degrade the delta-doped structure.

7. Summary

Delta-doped CCD technology enhances the UV response of thinned, backside-illuminated CCDs by using MBE to incorporate 30% of a monolayer of boron atoms 5 Å below the backside silicon crystal surface. With this technique, backside potential bands are permanently pinned, yielding devices with 100% internal quantum efficiency in the near UV and blue visible. The response of delta-doped CCDs is highly uniform and these devices have exhibited long-term stability. Compatibility of delta-doped CCD technology with antireflection coatings has been demonstrated by depositing HfO_2 on a delta-doped CCD, resulting in further enhancement of the total (external) quantum efficiency.

8. Acknowledgment

We thank A. Bauer for doing much of the work for the deposition of the HfO_2 layers at University of Arizona. The research described here was performed at the Center for Space Microelectronics Technology, Jet Propulsion Laboratory (JPL), California Institute of Technology, and was jointly sponsored by the National Aeronautics and Space Administration, Office of Space Science Instruments, Office of Technology and Applications Program, and the Department of Defense, Ballistic Missile Defense Organization.

REFERENCES

1. J.R. Janesick, J. Hyncek, and M.M. Blouke, SPIE Vol. 290, (1981).
2. J. Janesick, T. Elliot, G. Frascetti, S. Collins, M. Blouke, and B. Corrie, SPIE, Vol. 1071, "Optical Sensors and Electronic Photography", pp. 153-169 (1989).
3. M. Li, Hoenk, P.J. Grunthamer, F.J. Grunthamer, B.W. Terhune, M. Fattahi, and H-F Tseung, Appl. Phys. Lett., Vol. 61, pp. 1084-1086, 1992.
4. R. Winzenread, Proceedings of SPIE, Vol. 2198, "Astronomical Telescopes and Instrumentations for the 21st Century" (March 1994).
5. M. Lesser, Optical Eng. Vol. 26, pp. 911-915, (1987).